



DUAL SWITCH DC-DC HIGH GAIN CONVERTER

Mr. Althaf P K, PG Scholar

Dept of Electrical & Electronics Engg,
Mar Athanasius College of Engineering
Kothamangalam, Kerala, India

Prof. Beena M Varghese

Dept of Electrical & Electronics Engg,
Mar Athanasius College of Engineering
Kothamangalam, Kerala, India

Prof. Sija Gopinathan

Dept of Electrical & Electronics Engg,
Mar Athanasius College of Engineering
Kothamangalam, Kerala, India

Prof. Emmanuel Babu

Dept of Electrical & Electronics Engg,
Mar Athanasius College of Engineering
Kothamangalam, Kerala, India

Prof. Mohitha Thomas

Dept of Electrical & Electronics Engg,
Mar Athanasius College of Engineering
Kothamangalam, Kerala, India

Prof. Neema S

Dept of Electrical & Electronics Engg,
Mar Athanasius College of Engineering
Kothamangalam, Kerala, India

Abstract—For fuel cell vehicles, the DC-DC converter should have high efficiency, low voltage stress, small size, and high gain. Conventional two-, three-, and cascading boost converters, however, are unable to satisfy the specifications. The innovative non-isolated DC-DC converter with switched-inductor and switched-capacitor that is proposed in this study can achieve low voltage stresses across components, high gain, wide input voltage range, and common ground structure. This study analyzes the design of the component characteristics, the operating principle, and the comparisons with other high-gain converters. Lastly, findings from experiments and simulations confirm that the suggested topology works. MATLAB/SIMULINK is used to carry out the simulation. The experimental voltage input prototype has a voltage range of 25–80V. There is a 200V rated output voltage and a 100W rated power. The highest level of efficiency is 95% completed by using the pulse produced by the TMS320F28027F microcontroller with a TLP250H-constituted interface circuit. This converter can be used with fuel cell automobiles.

Index Terms—Boost Converter, Gain, Efficiency.

I. INTRODUCTION

An increasing amount of research is being done on the issue of excessive energy use and society's reliance on fossil fuels as nonrenewable resources like coal, oil, and gas become more rare [5]. The fuel cells have the ability to produce "clean" power with great efficiency and a high energy density by using either hydrogen or natural gas. However, the output voltage of fuel cells decreases noticeably as the output current increases, in contrast to batteries, which have a relatively constant output voltage. Therefore, to interface between the high voltage DC bus of the motor driving inverter and the low voltage fuel cell source, a step-up DC-DC converter with a wide range of voltage-gain is necessary. For stepping up voltage, one of the most used topologies is the traditional DC-DC Boost converter. Theoretically, the typical boost converter can obtain a significant voltage gain as the duty cycle approaches unity [4].

Researchers have suggested a wide range of topologies to achieve a DC-DC Boost converter with a high voltage gain

and minimal voltage stress. These converters fall into two categories: non-isolated and isolated. Theoretically, an infinitely large voltage-gain can be obtained by raising the turns ratio of the transformer used in isolated converters, which are widely utilized in many applications. Galvanic isolation is not always necessary, though, and the snubber circuit needed in an isolated topology will make the converter design more difficult. Non-isolated converters are less expensive and have fewer magnetic losses than isolated converters. One way to create a high voltage-gain in topology is to add a linked inductor, for example. The voltage stress across the power semiconductors can be cut in half by using the "switched-capacitor-based active-network" (SC-ANC), which also allows the voltages across the output capacitors to naturally balance. However, the circuit's leakage inductance could cause a significant voltage spike to appear on the power switches. The switched-capacitor circuit was examined because, rather than having a common ground structure, there is a diode located between the ground points of the input voltage source side and the load side. This diode allows for flexible voltage regulation, which is achieved by combining the circuit with other DC-DC converters. Nevertheless, the potential difference between the ground points of the input voltage source side and the load side is a high frequency PWM voltage. as a consequence, it could bring about problems related to the rate of change over time of the variable (du/dt) could restrict its use

To tackle these problems, a fresh non-isolated high ratio step-up converter is being implemented. This paper introduces a dc-dc converter design features that follows: It decreases the voltage pressure on the power devices, shares a similar base on both the input and output ends. Both power switches switch on and off at the same time. In the same manner Consequently, the management of the converter is uncomplicated, and authority is maintained, low on-state resistance switches can be used. The system works with a high voltage amplification and a broad input voltage range and avoids the use of any excessive values

for its operation.

II. METHODOLOGY

Two switches (S1 and S2), four diodes (D1, D2, D3, D4, and D5), two inductors (L1 and L2), and five capacitors (C1, C2, C3, C4, and C5) make up the new high gain boost converter. The revised high gain boost converter is depicted in Figure 1.

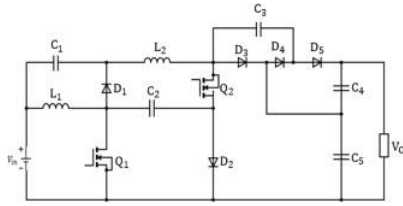


Fig. 1. High Gain Boost Converter

A. Modes of Operation

The continuous conduction mode (CCM) and the continuous bidirectional conduction mode (CBCM) are the two primary modes of operation for the suggested boost converter. The input inductor current, i_{L1} , runs continuously in a single direction in both modes. The rear-inductor current i_{L2} flows continuously in both CCM and CBCM, but it does so in a unidirectional manner in CCM and a bidirectional manner in CBCM.

1) *Mode 1*: Upon activating switch S, The switches S_1 and S_2 , as well as the diodes D_1 and D_4 , are switched on at mode 1, while the diodes D_2 , D_3 , and D_5 are turned off. The inductors L_1 and L_2 are currently charged via the source. It charges capacitor C_2 with capacitor C_1 . Both inductors' current rises linearly. The load is charged by the output capacitor C_3 . The mode 1 functioning circuit is displayed in Figure 2.

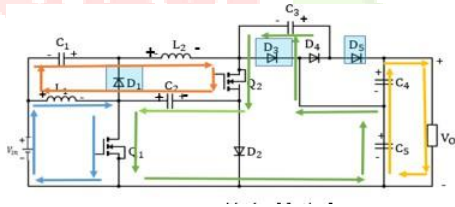


Fig. 2. Mode 1 Operating circuit

2) *Mode 2*: Diodes D_1 and D_4 , switches S_1 and S_2 , and diodes D_2 , D_3 , and D_5 are all turned off when switch S is turned off. Inductor L_1 and L_2 discharge and charge C_1 at this point, and inductor L_1 and L_2 , along with capacitor C_2 , charges capacitor C_3 and charge. The capacitor voltages V_{C1} and V_{C3} rise as a result, whereas V_{C2} falls. i_{L1} and i_{L2} both decrease linearly. The mode 2 functioning circuit is displayed in Figure 3.

Figure 4 shows the theoretical waveforms for mode 1 and mode 2.

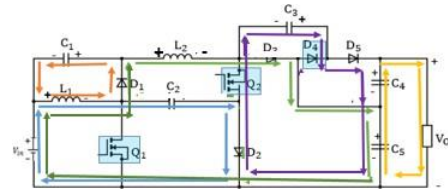


Fig. 3. Mode 2 Operating circuit

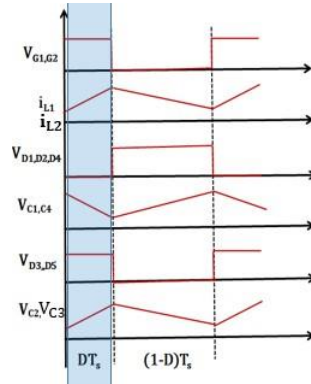


Fig. 4. Theoretical waveform

B. Component Design

$V_{in} = 25V$ is used as the input voltage. The output voltage and power are assumed to be $V_o = 200V$ and $P_o = 100W$. Time duration, $T_s = 1/f_s = 0.000020sec$, is determined by the switching frequency, $f_s = 20kHz$.

The following formula can be used to determine load resistance:

$$R_o = \frac{V_o^2}{P_o} = \frac{200^2}{100} = 400\Omega \quad (1)$$

Voltage Gain,

$$\frac{V_o}{V_{IN}} = \frac{3 + D}{(1 - D)^2} = 8 \quad (2)$$

Duty ratio,

$$D = 0.35 \quad (3)$$

For the inductors L_1 & L_2 , the following equations are used.

$$I_{L1} = \frac{2I_o}{1 - 2D} = \frac{2 * 0.5}{1 - 2 * 0.35} = 5.3A \quad (4)$$

$$L_1 \geq \frac{V_{IN} * D}{\Delta I_{L1} * f_s} = \frac{25 * 0.35}{1 - 2 * 0.35} \geq 0.3mH \quad (5)$$

It is approximated to 1 mH.

$$I_{L2} = \frac{2I_o}{1 - 2D} = \frac{2 * 0.5}{1 - 2 * 0.35} = 5.3A \quad (6)$$

$$L_2 \geq \frac{V_{IN} * D}{\Delta I_{L2} * f_s} = \frac{25 * 0.35}{3.34 * 20000} \geq 0.3mH \quad (7)$$

330μH is the selected value.

The following formulas are used to determine the values of capacitors.

$$C_1 \geq \frac{2D * I_0}{(1 - D) * \Delta V_{C1} * f_s} \quad (8)$$

$$C_2 \geq \frac{(1 + D) * I_0}{(1 - D) * \Delta V_{C2} * f_s} \quad (9)$$

$$C_3 \geq \frac{I_0}{\Delta V_{C3} * f_s} \quad (10)$$

$$C_4 \geq \frac{(1 + D) * I_0}{\Delta V_{C4} * f_s} \quad (11)$$

$$C_5 \geq \frac{D * I_0}{\Delta V_{C5} * f_s} \quad (12)$$

C_1, C_2, C_3, C_4 and C_5 are taken as $470 \mu F$

III. SIMULATIONS AND RESULTS

By selecting the values shown in Table 1, the high gain boost converter is simulated in MATLAB/SIMULINK. The MOSFET switch operates at a steady 20 kHz switching frequency. When the output power, P_o , is 100W, a dc input

TABLE I
SIMULATION PARAMETERS OF HIGH GAIN BOOST CONVERTER

Parameters	Specification
Input voltage V_{in}	25 V
Output voltage V_o	200 V
Inductor L_1	330 μH
Inductor L_2	1 mH
Capacitor C_1, C_2, C_3, C_4, C_5	470 μF
Switching frequency	20 kHz
Output load	400 Ω
Duty ratio	35 %

voltage, V_{in} , of 25V yields a dc output voltage, V_o , of 200V. The input voltage and current are displayed in Figure 5, while the output voltage and current are displayed in Figure 6. As a result, 8 is the voltage gain.

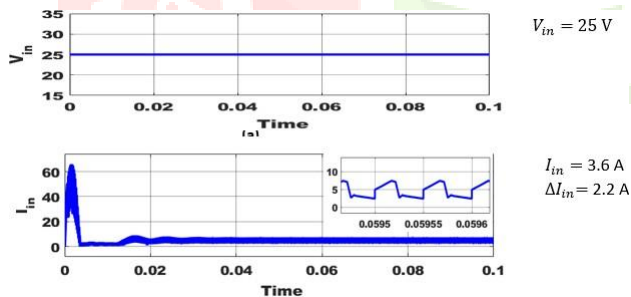


Fig. 5. (a) Input Voltage (V_{in}) and (b) Input Current (I_{in})

The gate pulse and voltage stress across the switch are depicted in Figures 7 and 8. The switch is under 37.8 V and 75.97 V of voltage stress, respectively.

Figure 8 illustrates the voltage across capacitors: $V_{C1} = 12.28$ V, $V_{C2} = 37.28$ V, $V_{C3} = 111.1$ V, $V_{C4} = 111.1$ V, & $V_{C5} = 75.97$ V. The current across inductances L_1 and L_2 is displayed in Fig. 9. The current over the filter inductances i_{L1} is 3.84 A, and i_{L2} is 1.08 A, as can be shown.

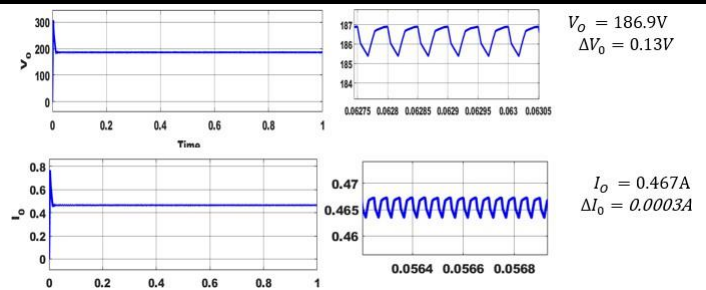


Fig. 6. (a) Output Voltage (V_o) and (b) Output Current (I_o)

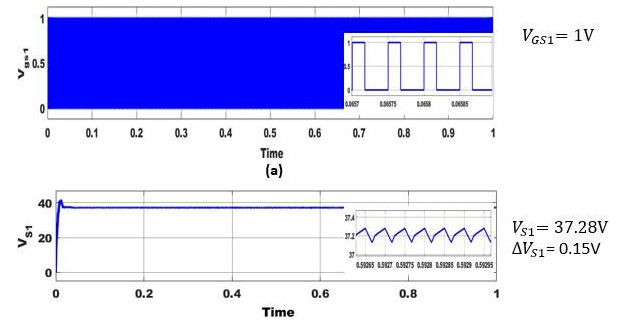


Fig. 7. Gate Pulse (V_{gs1}) and Voltage Stress (V_{s1}) of switch S_1

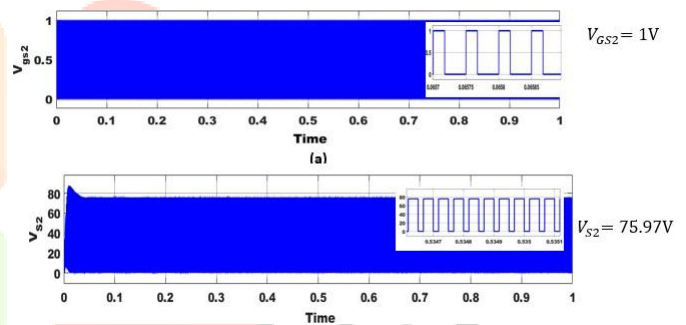


Fig. 8. Gate Pulse (V_{gs2}) and Voltage Stress (V_{s2}) of switch S_2

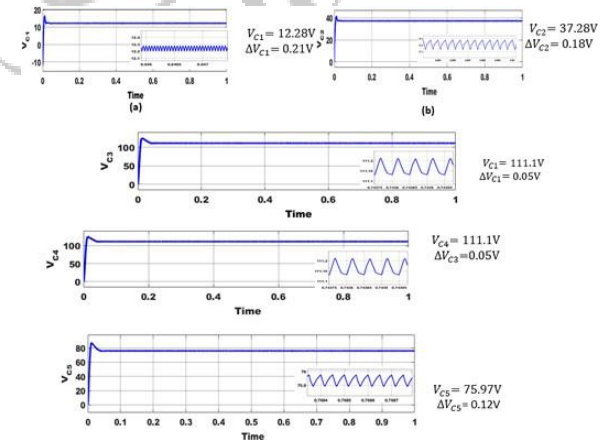
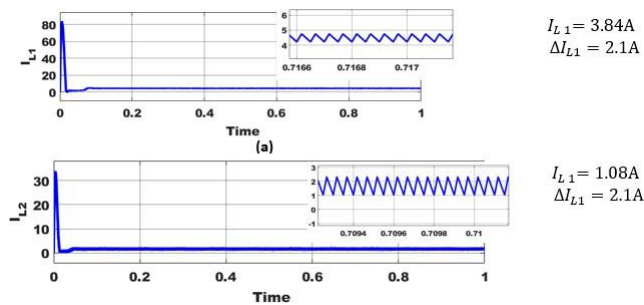


Fig. 9. Voltage across Capacitor (a) V_{C1} , (b) V_{C2} , (c) V_{C3} , (d) V_{C4} , (e) V_{C5}

Fig. 10. Current across Inductance (a) i_{L1} , (b) i_{L2}

IV. PERFORMANCE ANALYSIS

The efficiency of a power equipment at any load is determined by the power output to power input ratio. Here, Fig. 11 shows the efficiency of the high gain boost converter with R and RL loads as a function of output power. The maximum converter efficiency is 93.01% and 90.4% for R & RL load. The efficiency change with power output for both loads is moderate, at about 100 W. The high gain boost converter can therefore be used in medium power applications.

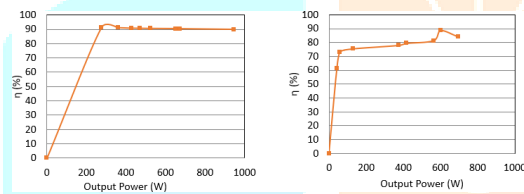


Fig. 11. Efficiency Vs Output Power for (a) R load (b) RL load

Figure 12 displays the high gain boost converter's gain plotted against duty ratio. As the duty ratio is changed, the gain rises.

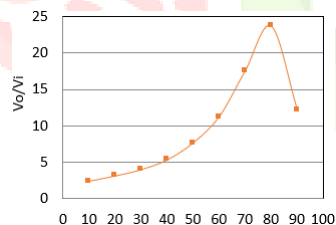


Fig. 12. Voltage gain VS Duty ratio

Figure 13 displays the high gain boost converter's output voltage ripple plotted against duty ratio.

Plotting the output voltage ripple for the modified boost converter against switching frequency is shown in Figure 14. There is less ripple in the output voltage as the switching frequency is increased.

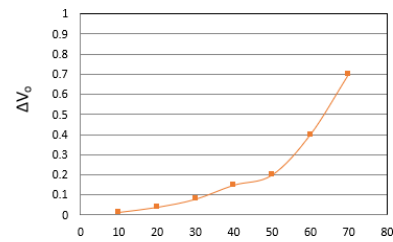


Fig. 13. Output Voltage Ripple VS Duty Ratio

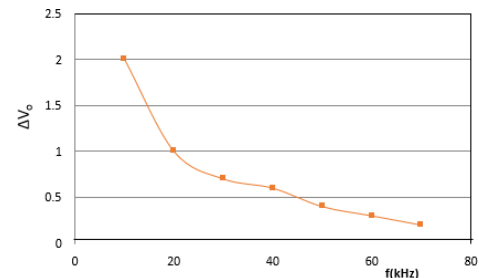


Fig. 14. Output voltage ripple VS frequency

V. COMPARITIVE STUDY

Table 2 compares the suggested high gain boost converter with a high gain boost converter with the same input voltage and switching frequency. The comparison shows that the gain increases from 4.35 to 8 with the same input voltage of 25V and switching frequency of 20kHz. However, the suggested converter has larger output voltage and current ripple.

TABLE II
COMPARISON BETWEEN HIGH GAIN BOOST CONVERTERS & PROPOSED TRANSFORMERLESS BOOST CONVERTER

Parameters	Boost Converter	Modified Converter
No. of Switches	2	2
No. of Inductor	1	2
No. of Capacitor	4	3
Voltage Gain	4.35	13
Efficiency	90%	95.2%
Output Voltage Ripple	0.01	0.13V
Output Current Ripple	0.002	0.0003A
Voltage Stress across Switches	$V_{S1}=78.9V$ $V_{S2}=81.14V$	$V_{S1}=39.28V$ $V_{S2}=75.97V$

The component-by-component comparison of the suggested high gain boost converter with other converters is displayed in Table 3. The components utilized in the various converters serve as the basis for comparison.

TABLE III
COMPARISON BETWEEN HIGH GAIN BOOST CONVERTER & OTHER CONVERTERS

Converters	Proposed Converter	Boost Converter	Quadratic Boost Converter	Quasi-Z-Boost Converter
Switches	2	2	1	1
Inductors	2	1	2	2
Capacitors	5	4	2	3
Diodes	5	5	3	2

VI. SETUP FOR EXPERIMENT WITH RESULTS

The input voltage is lowered to 2V for hardware implementation, and the TMS320F28335 processor is used to generate the switching pulses. MOSFET IRF3105 is the switch in use. The TLP250H optocoupler, which is utilized to isolate and shield the microcontroller from harm and to provide the necessary gating to turn on the switches, is used in the driver circuit.

Fig. 15 depicts the experimental configuration of a high gain boost converter. The DC source provides a 2V, 0.4A DC power for the input. The TMS320F28335 microcontroller sends switching pulses to the driving circuit. Thus, the power circuit depicted in Figure 15 yields an output voltage of 10.6V. The DSO oscilloscope is used to measure output voltage of the converter.



Fig. 15. Experimental Setup

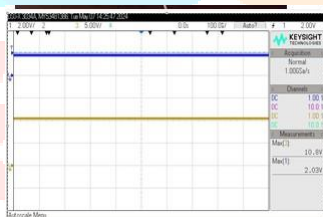


Fig. 16. Output Voltage of High Gain Converter

VII. CONCLUSION

A new increased gain boost converter with reduced voltage stress is implemented. This construction combines a voltage multiplier cell with a switching inductor. The suggested converter provides high gain and less voltage stress across the switching components in comparison to conventional boost DC-DC converters. Analysis and simulation of the suggested converter are done. The simulation shows that, with an output power of 100W, the converter achieves an efficiency of 93.01%. Other benefits of the suggested topology include a broad duty ratio operating range, no transient current, and common ground. The TMS320F28027F microcontroller is used to implement the control of the suggested converter. With an output voltage of 72V, the 20W converter prototype performs as expected when taking component drops into account. Because of these characteristics, the topology that is being shown is a great interface for photovoltaic applications.

REFERENCES

- [1] Ling Qin, Lei Zhou, Waqas Hassan, John Long Soon, Min Tian and Jiapeng Shen, "A Family of Transformer-Less Single-Switch Dual-Inductor High Voltage Gain Boost Converters with Reduced Voltage and Current Stresses, ", IEEE Transactions on Power Electronics, Vol. 36, No. 5, May 2021
- [2] A. Kumar et al., "A High Voltage Gain DC-DC Converter With Common Grounding for Fuel Cell Vehicle," in IEEE Transactions on Vehicular Technology, 2020
- [3] M. Veerachary and P. Sen, "Dual-Switch Enhanced Gain Boost DC-DC Converters," in IEEE Transactions on Industry Applications, vol. 58, no. 4, pp. 4903-4913, July-Aug. 2022
- [4] G. Dotelli, R. Ferrero, P. G. Stampino, S. Latorrata, and S. Toscani, "PEM fuel cell drying and flooding diagnosis with signals injected by a power converter," IEEE Trans. Instrum. Meas., vol. 64, no. 8, pp. 2064-2071, Aug. 2015.
- [5] B. Zeng, J. Zhang, X. Yang, J. Wang, J. Dong, and Y. Zhang, "Integrated planning for transition to low-carbon distribution system with renewable energy generation and demand response," IEEE Trans. Power Syst., vol. 29, no. 3, pp. 1153-1165, May 2014.
- [6] Sajad Rostami, V. Abbasi and T. Kerekes, "Switched capacitor based Z-source DC-DC converter", IET Power Electronics, vol. 12, no.13, pp. 3582-3589, 2019
- [7] X. Wu, M. Yang, M. Zhou, Y. Zhang and J. Fu, "A Novel High-Gain DC-DC Converter Applied in Fuel Cell Vehicles," in IEEE Transactions on Vehicular Technology, vol. 69, no. 11, pp. 12763-12774, Nov. 2020
- [8] S. Gao, Y. Wang, Y. Liu, Y. Guan, and D. Xu. A novel DCM soft-switched SEPIC-based high-frequency converter with high step-up capacity. IEEE Trans. Power Electron, Oct. 2020
- [9] Minh-Khai Nguyen, T. Duong, Y. Lim, "Switched-Capacitor-Based Dual-Switch High-Boost DC-DC Converter", IEEE Transactions on Power Electronics, 2018, vol. 33, no. 5, pp. 4181-4189, May 2018